DOI: 10.26599/FSHW.2026.9250972

Contents lists available at SciOpen

Food Science and Human Wellness

journal homepage: https://www.sciopen.com/journal/2097-0765

China Food Publishing Co.

Chimonanthus salicifolius S. Y. Hu. leaves flavonoids alleviate alcoholic liver disease by activating the Nrf2/HO-1 signaling pathway and maintaining intestinal homeostasis

Siqi Li, Hui Chen, Lingli Chen, Wenbing Hu, Suyun Lin, Wenjun Wang*

Jiangxi Key Laboratory of Natural Products and Functional Food, College of Food Science and Engineering, Jiangxi Agricultural University, Nanchang 330045, China

ABSTRACT: Alcoholic liver disease (ALD) is thought to be primarily caused by oxidative damage and disruption of intestinal homeostasis. This study aimed to examine the protective effects of *Chimonanthus salicifolius* S. Y. Hu. leaves flavonoids (CLFs) against ALD and explore the underlying mechanisms based on hepatic oxidative stress, inflammation, intestinal barrier function and non-targeted metabolomics. The results indicated that CLFs improved the condition of mice with alcoholic liver disease and restored normal liver function. Through a combination of biochemical assays, non-targeted metabolomics, and gut microbiota analysis, we found that CLFs regulated glutathione metabolism and the tryptophan metabolic pathways, and activated the Nrf2/HO-1 signaling pathway, thus alleviating oxidative stress levels. Additionally, by regulating the composition of the gut microbiota and preserving intestinal barrier function, CLFs led to a decrease in harmful microorganisms like *g-Sutterella* and an increase in helpful microbes like *g-Clostridium-f-Clostridiaceae*. In summary, these findings provide a scientific basis for considering CLFs in the treatment of alcoholic liver disease.

Keywords: *Chimonanthus salicifolius* S. Y. Hu., Flavonoids, Alcoholic liver disease, Gut–liver axis, Non-targeted metabolomics

1. Introduction

Alcoholic liver disease is a liver disease caused by excessive alcohol consumption[1]. It frequently starts with an accumulation of fat in the liver, which can lead to cirrhosis, fatty degeneration, inflammation, liver fibrosis, and possibly even liver cancer[2]. Nowadays, alcoholic beverages are often consumed during social activities or as a means of stress relief, but their detrimental effects on health are frequently disregarded. According to the survey, the mortality rate of ALD increased from 6.71 cases per 100000 people to 12.53 cases between 1999 and 2022, with a significant acceleration between 2018 and 2022[3]. ALD is responsible for approximately 5.9% of global deaths related to liver disease and poses a significant economic challenge[4]. As a result, alcoholic liver disease is now recognized as one of the most prevalent illnesses that seriously

***Corresponding author**
wwjun9999@jxau.edu.cn

Received 29 September 2025
Received in revised from 10 November 2025
Accepted 6 January 2026

endanger global public health, affecting people's physical well-being and impeding societal advancement in numerous nations.

Occurrence of alcoholic liver disease is associated with oxidative stress, inflammatory responses, intestinal flora imbalance, and metabolic disorders[5]. Oxidative stress is the primary cause of ALD. Exposure to alcohol raises oxidant levels and hinders the body's ability to get rid of free radicals, which causes an imbalance that is mostly caused by reactive oxygen species. The liver exhibits structural and functional abnormalities as a result of this imbalance in the oxidation-antioxidation system[6]. Additionally, excessive alcohol consumption can stimulate the intestines, damage the intestinal barrier and alter mucosal permeability[7]. Intestinal damage allows intestinal endotoxins to enter the portal vein circulation and promotes the transfer of bacterial products from the intestine to the liver. Consequently, this process induces the production of pro-inflammatory factors and further encourages the progression of ALD[8]. As the main organ for amino acid metabolism, the liver is rich in enzyme content, leading to an active change in amino acid metabolism. When there is liver injury or pathological change, amino acid metabolism in liver cells decreases on account of the liver function being presented with an obstacle, which brings about a rise in the concentration of amino acid in the blood and a lack of it in the body[9]. Studies have shown that alcohol stimulation can affect tryptophan metabolism and glutathione metabolism pathways in the liver[10-11]. Once the liver is damaged, it can also lead to metabolic disorders such as lactic acidosis[12], hypoalbuminemia[13] and malabsorption of fat[14]. However, there are limited drugs available for the treatment of alcoholic liver disease, and most drugs have harmful side effects[15]. Abstinence from alcohol, corticosteroids, and nutritional supplementation has been considered a conventional clinical treatment strategy for ALD[16]. There is an evidence that flavonoids have positive effects on lipid metabolism, oxidative stress, inflammation, insulin resistance, cell apoptosis, cell proliferation, tumors, and hippocampal brain-derived neurotrophic factor, thereby benefiting non-alcoholic/alcohol-induced liver disease, type II diabetes, cardiovascular disease, cancer, memory and cognition[17-19]. Given these benefits, natural flavonoids are considered to have significant potential for liver treatment.

C. salicifolius, commonly known as golden tea or fragrant wind tea, belongs to the *Chimonanthus* genus. This plant is peculiar to China and is mostly found in the provinces of Jiangxi, Zhejiang, Hunan, Anhui, and Fujian[20]. *C. salicifolius* has a variety of active ingredients, including flavonoids, polysaccharides, volatile oils, and alkaloids, in addition to essential minerals. According to studies, *C. salicifolius* has antibacterial qualities, regulates the immune system, protects the liver, lowers uric acid levels, controls sugar and lipid metabolism, and increases antioxidant capacity[21-23]. Nevertheless, limited studies are exploring the protective effects of flavonoids derived from the leaves of *C. salicifolius* on alcoholic liver disease (ALD), particularly in relation to the gut-liver axis.

This study primarily evaluated the therapeutic effects of *C. salicifolius* leaves flavonoids on ALD mice, exploring their protective mechanisms through liver oxidative stress, inflammation, intestinal barrier function,

non-targeted metabolomics, and gut microbiota, thereby providing new insights for the development of natural and safe hangover-relief and liver-protective health products.

2. Materials and methods

2.1 Materials

C. salicifolius leaves were purchased from Lishui City, Zhejiang Province, China. Bifendate was purchased from Wandebang Pharmaceutical Group Co., Ltd. Lieber-DeCarli liquid feed (TP4030D, TP4030C) was purchased from Trophic Animal Feed High-Tech Co., Ltd. (Nantong, China). Diagnostic kits for detecting total cholesterol (TC), thyroglobulin (TG), alanine aminotransferase (ALT), aspartate transaminase (AST), malondialdehyde (MDA), superoxide dismutase (SOD), and glutathione (GSH) were purchased from Nanjing Jiancheng Biological Engineering Research Institute (Nanjing, China). A diagnostic kit for detecting total antioxidant capacity (T-AOC) was purchased from Beyotime Biotechnology Co., Ltd. (Shanghai, China). Enzyme linked immunosorbent assay (ELISA) kits for tumor necrosis factor-α (TNF-α), interleukin-6 (IL-6), IL-1β, and IL-10 were purchased from Jiangsu Enzyme Immunoassay Technology Bio-Pharmaceutical Co., Ltd. (Jiangsu, China). The primary and secondary antibodies related to nuclear factor erythroid 2-related factor 2 (Nrf2, 1:12000 dilution), heme oxygenase 1(HO-1, 1:6000 dilution), and β-actin (1:10000 dilution) were purchased from Proteintech (Wuhan, China). All other reagents (analytical grade) used in this study were purchased from local suppliers.

2.2 Methods

2.2.1 Preparation of CLFs

The preparation method of *C. salicifolius* leaves flavonoids was referenced from Chen et al. [24] with some modifications. After being crushed, dried leaves of *C. salicifolius* were sieved through a 60 mesh. The specific extraction conditions are as follows: 60% ethanol concentration, 60 min of ultrasonic treatment time, 40 ℃extraction temperature, 1:20 (g/mL) solid-liquid ratio, and 1500 W ultrasonic power. The filtrates were mixed following two rounds of ultrasonication, and centrifugation at 4000 r/min was used to extract the crude extract. The crude extract underwent a gradient elution process using water, 40% ethanol, 70% ethanol, and 95% ethanol after being freeze-dried and adsorbed using HPD100A macroporous resin. After being collected, the 40% ethanol eluate was freeze-dried to create a powder. It was confirmed to be CLFs with a total flavonoid concentration of 79.95% ± 3.54%.

2.2.2 HPLC Analysis of CLFs

Flavonoids were identified and quantified using an Agilent HPLC system equipped with a UV-vis detector and a C_{18} column (250 mm × 4.6 mm, 5 μm, Waters, Ireland). Before use, dissolve the sample in methanol and filter it through a microporous nylon membrane (0.22 μm). The mobile phase consists of 0.1% (v/v) acetic acid aqueous solution (solvent A) and acetonitrile (solvent B). The experimental conditions were based on Chen [24] with some modifications. The flow rate was 1 mL/min; the column temperature was 40℃; and the UV detection wavelength was set at 254 nm.

2.2.3 Antioxidant Capacity of CLFs in Vitro

The 1,1-diphenyl-2-picrylhydrazyl (DPPH) radical (DPPH•), 2,2-azino-bis(3-ethylbenzothiazoline-6-sulfonic acid (ABTS) radical (ABTS+), and the total reducing capacity of CLFs were measured according to the method reported by Meng et al[25].

2.2.4 Animal Experiments

All the animal experiments were approved by the Animal Cared Use Committee of Jiangxi Agricultural University (JXAUA01) and carried out in accordance with the Guide for the Care and Use Laboratory Animals. Sixty male C57BL/6J mice (SCXK (Yu) 2020-0005) aged 7-8 weeks were purchased from Henan Skebes Biotechnology Co., Ltd. (Henan, China), and housed under stable and specific pathogen-free conditions (temperature: 23℃ ± 1℃, humidity: 50% ± 10%, in a 12h light/dark cycle), with free access to food and water.

This modeling method refers to the NIAAA model[26]. After a 5-day acclimatization period with standard chow (ad libitum diet and water), mice were randomly assigned to groups (n=10), including the normal control group (NC), model control group (MC), positive control group (PC, 150 mg/kg bifendate), low-dose drug treatment group (CLFs-L, 100 mg/kg CLFs), medium-dose drug treatment group (CLFs-M, 200 mg/kg CLFs), and high-dose drug treatment group (CLFs-H, 300 mg/kg CLFs). After a 5-day adaptation period using a graded feeding method (ad libitum diet, no water provided), formal modeling was initiated. The NC group was administered the Lieber DeCarli control liquid diet, while all other groups received the Lieber DeCarli alcohol liquid diet containing 5% (v/v) ethanol. During the modeling period, the NC and MC groups were given distilled water via gastric lavage, whereas the PC and drug treatment groups received varying doses of the mixed solution as previously described. All groups were provided with an isocaloric diet daily to ensure energy intake balance. On the evening of day 10 of modeling, fasting was initiated. The following morning, between 7 and 9 a.m., except for the NC group, mice were administered a 31.5% (v/v) alcohol solution via gastric lavage, while the NC group received a 45% (w/v) dextrin solution via gastric lavage. Mice were euthanized 9 h later, and the required tissue samples were collected.

2.2.5 Serum and Hepatic Biochemical Analysis

Use the appropriate commercial kits to detect the levels of ALT, AST, TG, TC, MDA, SOD, GSH, and T-AOC in serum and liver tissue. Use ELISA kits to measure the levels of TNF-α, IL-6, IL-1β, and IL-10 in liver and colon tissue.

2.2.6 Histological Analysis

Liver and ileum tissue samples were immersed in 4% paraformaldehyde. Liver tissue was stained with hematoxylin and eosin (H&E) staining, and colon tissue was stained with periodic acid-schiff (PAS) staining. All samples were then examined under an optical microscope according to a modified reporting method.

2.2.7 Metabonomic Analysis

Weigh 30 mg of mouse liver samples (n=6), grind them, and add 800 μL of methanol: acetonitrile (1:1, v/v) solution. Ultrasound the mixture for 30 min, then freeze it at -20℃ for 30 min to pre-precipitate the proteins. Centrifuge at 4℃ at 12,000 r/min for 10 min, then take 800 μL of the supernatant, vacuum concentrate to dryness, add 150 μL of 50% methanol (containing 5 ppm 2-chlorophenylalanine) to resuspend, vortex for 30 s; centrifuge at 4℃ at 12,000 r/min for 10 min, transfer the supernatant through a 0.22 μm filter membrane, and add the filtrate to the detection vial for LC-MS/MS analysis. Mix 10-20 μL of each sample filtrate to form a quality control（QC） sample for evaluating instrument stability and data reliability.

The HPLC system (Vanquish Flex, Thermo) equipped with an ACQUITY UPLC HSS T3 column (100 A, 1.8 μm, 2.1 mm × 100 mm) was used in combination with a mass spectrometer (Orbitrap Exploris 120, Thermo). The mobile phase consists of 0.1% formic acid in water, and the mobile phase consists of acetonitrile (containing 0.1% formic acid). The column temperature is maintained at 40℃, the sample injection volume is 2 μL, and the flow rate is set to 0.4 mL/min.

Thermo Orbitrap Exploris 120 mass spectrometer under the control of Xcalibur software (version: 4.7, Thermo). Using the HESI source, the spray voltage was set to 3.5 kV/-3.0 kV, the sheath gas to 40 arb, the auxiliary gas to 10 arb, the capillary temperature to 320℃, the auxiliary gas temperature to 300℃, the primary resolution to 60,000, scan range 70-1000 m/z, AGC Target Standard, Max IT 100 ms, screening the top 4 ions for secondary fragmentation, dynamic exclusion time 4 s, secondary resolution 15,000, HCD collision energy 30%, AGC Target Standard, Max IT Auto.

2.2.8 16S rRNA-based Microbial Community Analysis

After euthanizing the mice, collect samples of cecal contents into sterile cryogenic tubes and immediately freeze them in liquid nitrogen for microbial DNA extraction. Use specific primers to amplify the V3/V4 hypervariable regions of bacterial 16S rRNA. Data analysis was performed using the Personal Gene Cloud Platform (Shanghai Personal Bio-Technology Co., Ltd., China). α diversity and β diversity of intestinal microbiota in each group of mice, as well as differences at the phylum and genus levels among the groups, were analyzed. Principal coordinate analysis (pCoA) was used to assess the similarity and differences in community composition among the groups.

2.2.9 Reverse Transcription Quantitative Polymerase Chain Reaction (RT-qPCR) Analysis

RT-qPCR analysis was used to detect the mRNA expression levels of Kelch-like ECH-associated protein 1 suppressor (Keap1), nuclear factor erythroid 2-related factor 2 (Nrf2), NADPH: quinone oxidoreductase 1 (NQO-1), heme oxygenase 1 (HO-1), toll-like receptor 4 (TLR4), and myeloid differentiation primary response protein 88 (MyD88) in liver tissue, and zonula occluden-1 (ZO-1), Occludin1, and mucin2 (MUC2) in colon tissue. Total RNA was extracted from mouse liver and colon tissues using the TransZol Up Plus RNA Kit according to the manufacturer's instructions. The primers used in this study were listed in Table 1. The specific operation steps refer to the previously reported method[27]. Target gene expression was normalized to β-actin gene levels and calculated using the $2^{-\Delta\Delta Ct}$ method.

Table 1 Primer sequences of RT-qPCR.

Primer Name	Forward	Reverse
Keap1	5'-GCCCAATTCATGGCTCACAA-3'	5'-GACCTTAGGGTGGATGCCTT-3'
Nrf2	5'-TCCCAGCAGGACATGGATTT-3'	5'-GGCCTTCTCCTGTTCCTTCT-3'
NQO-1	5'-TTCCCATTGCAGTGGTTTGG-3'	5'-TGGAAAGGACCGTTGTCGTA-3'
HO-1	5'-TGTCTGAGGCCTTGAAGGAG-3'	5'-CAGGGCCGTGTAGATATGGT-3'
TLR4	5'-GTTCTCTCATGGCCTCCACT-3'	5'-GTTCTCTCATGGCCTCCACT-3'
MyD88	5'-GCATGGTGGTGGTTGTTTCT-3'	5'-AACCGCAGGATACTGGGAAA-3'
ZO-1	5'-CCAGAGCCTCAGAAACCTCA-3'	5'-GCAGGAAGATGTGAAGAAGG-3'
Occludin 1	5'-GCGGAAAGAGTTGACAGTCC-3'	5'-GCAGGAAGATGTGCAGAAGG-3'
MUC-2	5'-TGTGGTCTGTGTGGGAACTT-3'	5'-GCTTACATCTGGGCAAGTGG-3'
β-actin	5'-GCTCCTGGCTCCTAGCACCAT-3'	5'-GCCACCGATCCACACAGAGT-3'

2.2.10 Western Blotting Analysis

Western blotting was used to detect the relative expression levels of Nrf2 and HO-1 proteins in liver tissue. Mouse liver tissue (50-100 mg) was homogenized in RIPA lysis buffer and centrifuged at 12,000 r/min at 4℃ for 10 min to extract total protein. Protein quantification of the supernatant was performed using the bicinchoninic acid (BCA) protein assay kit. Protein samples of uniform concentration were thoroughly mixed with loading buffer and denatured at 95℃ in a boiling water bath for 10 min. Proteins in the samples were separated on sodium dodecyl sulfate polyAcrylamide gel electrophoresis (SDS-PAGE) gels and transferred to polyvinylidene fluoride (PVDF) membranes[28]. Block the membrane with rapid blocking solution, incubate with the primary antibody for 1.5 h, then incubate with the secondary antibody for 1 h. Visualize the protein bands using enhanced chemiluminescence (ECL) reagents and the Gene Genius bioimaging system (Bio-Rad Laboratories, USA). Analyze the integral density of the protein bands using Image J.

2.2.11 Statistical Analysis

Statistical analysis was performed using SPSS Statistics 26 (SPSS Inc., Chicago, IL, U.S.A). Data were analyzed using one-way analysis of variance (ANOVA) and Duncan's multiple range tests to compare differences between groups. Experimental results are expressed as mean ± standard error (M ± SE). Significant differences were set at $P < 0.05$. Origin software (Origin, Farmington, ME, USA) was used to plot graphs.

3. Results

3.1 Content Analysis of CLFs

The components of CLFs were analyzed both qualitatively and quantitatively using HPLC. According to the findings, rutin, hyperoside, isoquercitrin, luteoloside, kaempferol-3-O-rutinoside and astragalin were the primary constituents of CLFs (Figure 1). The quantitative results of CLFs are shown in Table 2.

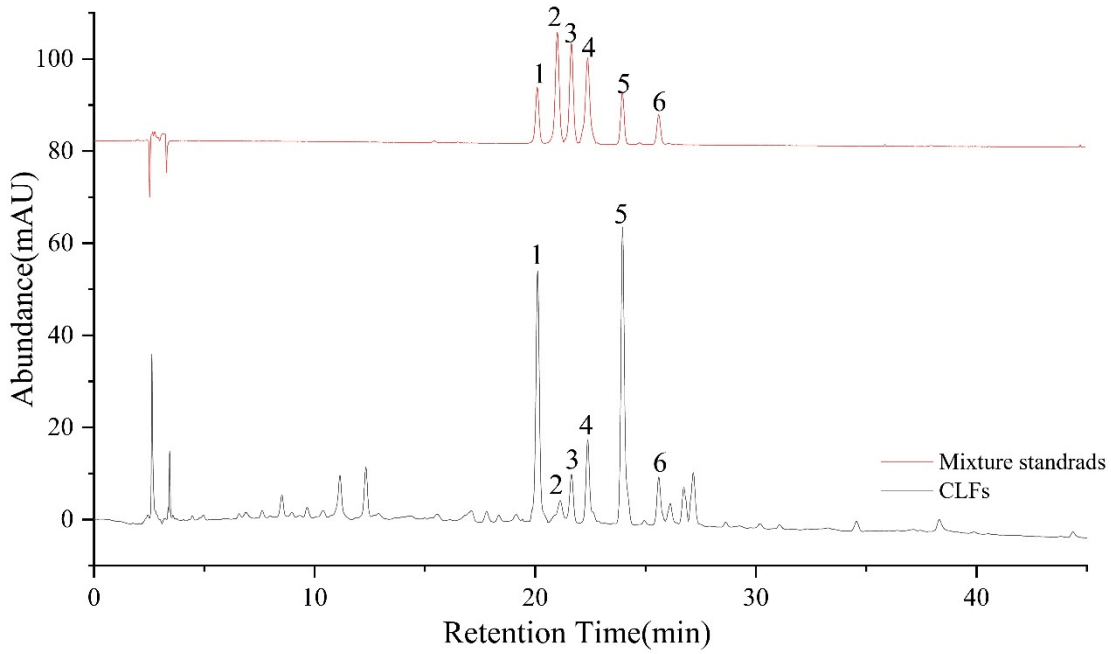

Figure 1 The HPLC profile of CLFs and mixture standards. Rutin (1); Hyperoside (2); Isoquercitrin (3); Luteoloside (4); Kaempferol-3-O-rutinoside (5); Astragalin (6).

Table 2 Components and contents of flavonoids in CLFs. Results are expressed as mean ± SE (n = 3).

Compounds	Calibration curve	R2	Tentative identification(μg/mg)
Rutin	y=17.985x+38.794	0.9966	37.15 ± 0.13
Hyperoside	y=29.023x+15.236	0.9956	1.38 ± 0.16
Isoquercitrin	y=23.71x-18.464	0.9962	6.01 ± 0.16
Luteoloside	y=23.383x-43.388	0.9973	9.30 ± 0.02
Kaempferol-3-O-rutinoside	y=19.882x-30.611	0.9964	39.21 ± 0.74
Astragalin	y=10.366x-19.408	0.9910	13.89 ± 0.10

3.2 Antioxidant Activity of CLFs

Total reduction capacity tests and free radical elimination assays (DPPH• and ABTS+) were used to assess the antioxidant activity of CLFs. The antioxidant capacity of CLFs is illustrated in Figure 2. As the concentration increases, the free radical removal capacity of CLFs continues to rise, and when the concentration reaches a certain level, its antioxidant capacity is comparable to that of vitamin C. Within the concentration ranges 32.5 to 1000 μg/mL, the total reducing capacity of CLFs continues to increase and demonstrates a dose-dependent relationship. These results indicate that CLFs possess good antioxidant capacity.

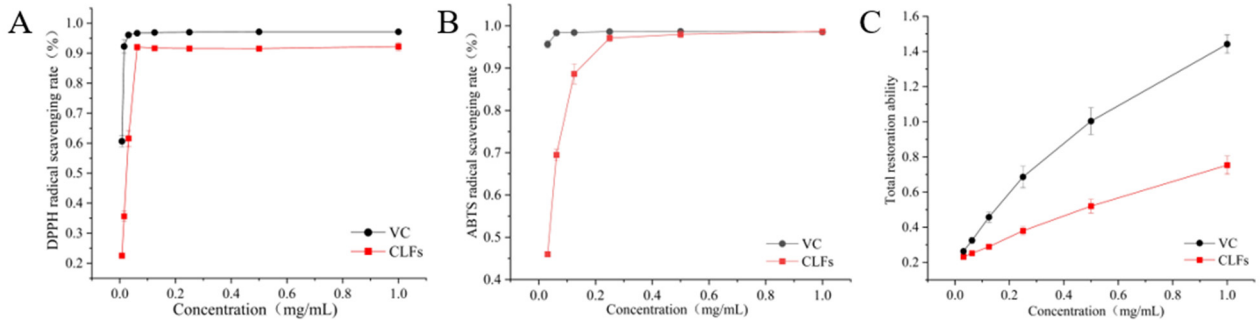

Figure 2 Antioxidant activities of CLFs *in vitro*. (A) DPPH radical scavenging activity; (B) ABTS radical scavenging activity; (C) Total reduction capacity. Vitamin C (VC) was used as a positive control. Results are expressed as mean ± SE (n = 3).

3.3 CLFs Improve Biochemical and Pathological Changes in ALD Mice

The variations in body weight during the modeling period are depicted in Figure 3B. As shown, all mice experienced a decrease in body weight following alcohol intake. The MC group's body weight dropped by 5.57% in comparison to the NC group. Nevertheless, this weight loss was lessened by oral administration of several concentrations of CLFs; the CLFs-L group had the greatest impact, with a body weight fall of only 2.44%. Additionally, the mice in the MC group had enlarged livers (Figure 3C) and atrophied spleens (Figure 3D), as evidenced by the substantial differences in their liver and spleen indices when compared to the NC group ($P < 0.05$). This implies that drinking alcohol caused physical harm to the mice. Significantly, CLFs supplementation reduced the severity of this damage, with the CLFs-H group showing the best response, underscoring CLFs' potent regulatory ability on the organ indices in mice.

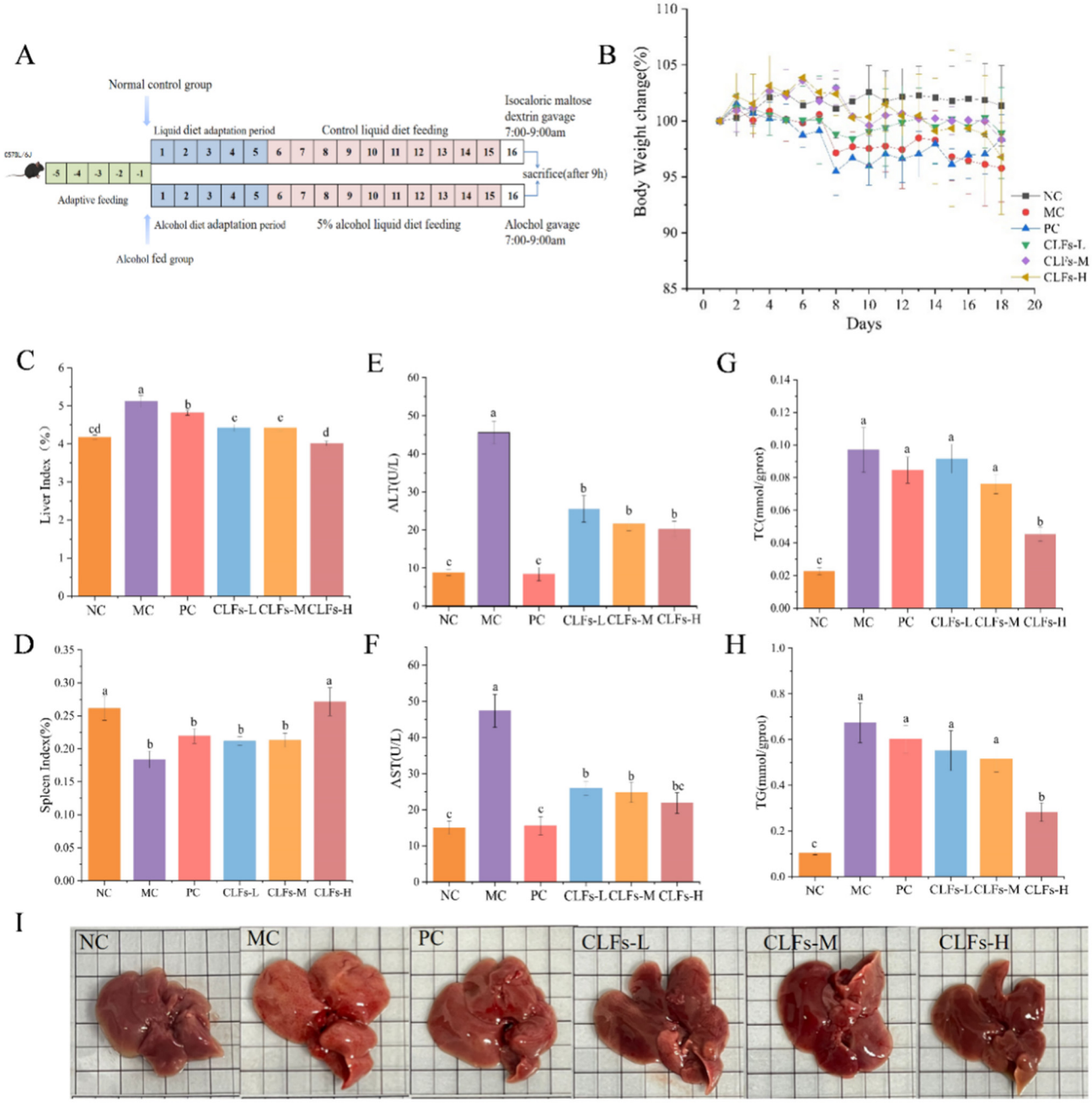

J

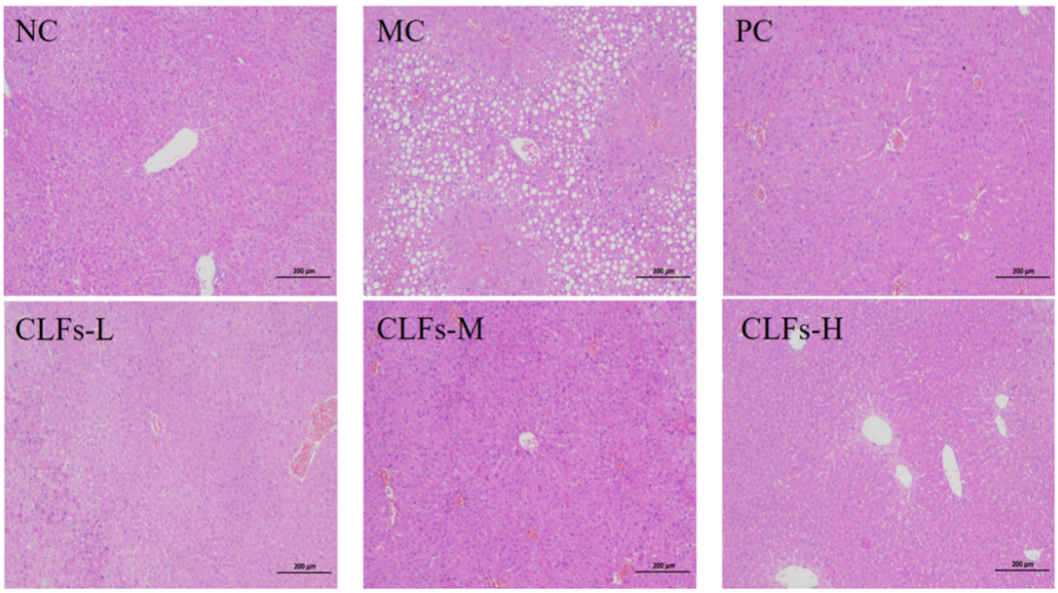

Figure 3 CLFs alleviate liver damage in ALD mice. (A) Animal experiment design; (B) Changes in mouse body weight; (C) Liver index; (D) Spleen index; (E) Serum ALT; (F) Serum AST; (G) Liver TC; (H) Liver TG; (I) Hepatological observations of ALD mice; (J) H&E staining (100×, scale bar: 200 μm). Bar charts marked with different letters indicate significant differences among the six groups ($P < 0.05$), results are expressed as mean ± SE (n = 6).

Research has demonstrated that serum enzyme levels are closely linked to the progression of alcoholic liver disease. The mice in the MC group had considerably higher serum ALT and AST levels (Figure 3E-F) than those in the NC group ($P < 0.05$), which suggests successful modeling. The mice's increased serum ALT and AST activity were successfully suppressed by the CLFs and bifendate intervention ($P < 0.05$). The results indicate that CLFs can effectively reverse alcohol-induced liver dysfunction, thereby alleviating alcohol-induced liver damage. Furthermore, as shown in Figures 3G and 3H, mice in the MC group had significantly higher ($P < 0.05$) levels of TC and TG in their livers, whereas supplementing with CLFs resulted in varying degrees of reduction in these levels. This suggests that CLFs intervention can alleviate alcohol-induced lipid metabolism dysfunction and reduce fat accumulation brought on by alcohol intake.

The anatomical observations of the livers of mice in each group are illustrated in Figure 3I. The livers of mice in the NC group were soft, smooth, and exhibited a normal reddish-brown color. In contrast, the livers of mice in the MC group were lighter in color, with enlarged tissue and granular elevations on the surface. Following the CLFs intervention, the liver condition of the mice was comparable to that of the NC group, both exhibiting a healthy reddish-brown color, with reduced granular elevations on the surface, and a significantly smaller volume compared to the MC group, consistent with the previous liver index results. A further pathological examination of the liver tissue (Figure 3J) revealed that the liver lobule structure in the NC group was intact, with uniform hepatocyte morphology, orderly arrangement, and clearly defined nuclei. However, alcohol intervention resulted in significant fat degeneration, the appearance of numerous fat droplets, and the disordered arrangement of liver cells. These damages were lessened following CLFs supplementation, mostly as a result of a decrease in lipid vacuoles, suggesting that CLFs can considerably lessen the pathological harm brought on by alcohol-induced liver disease in mice.

3.4 CLFs Reduce Oxidative Stress Levels and Liver Inflammation Levels in ALD Mice

SOD, GSH, and T-AOC levels were considerably lower ($P < 0.05$) in the MC group and MDA levels were significantly higher ($P < 0.05$) compared to the NC group. However, these changes were reversed after CLFs intervention (Figure 4A-D), indicating that CLFs supplementation helps restore the antioxidant system's balance.

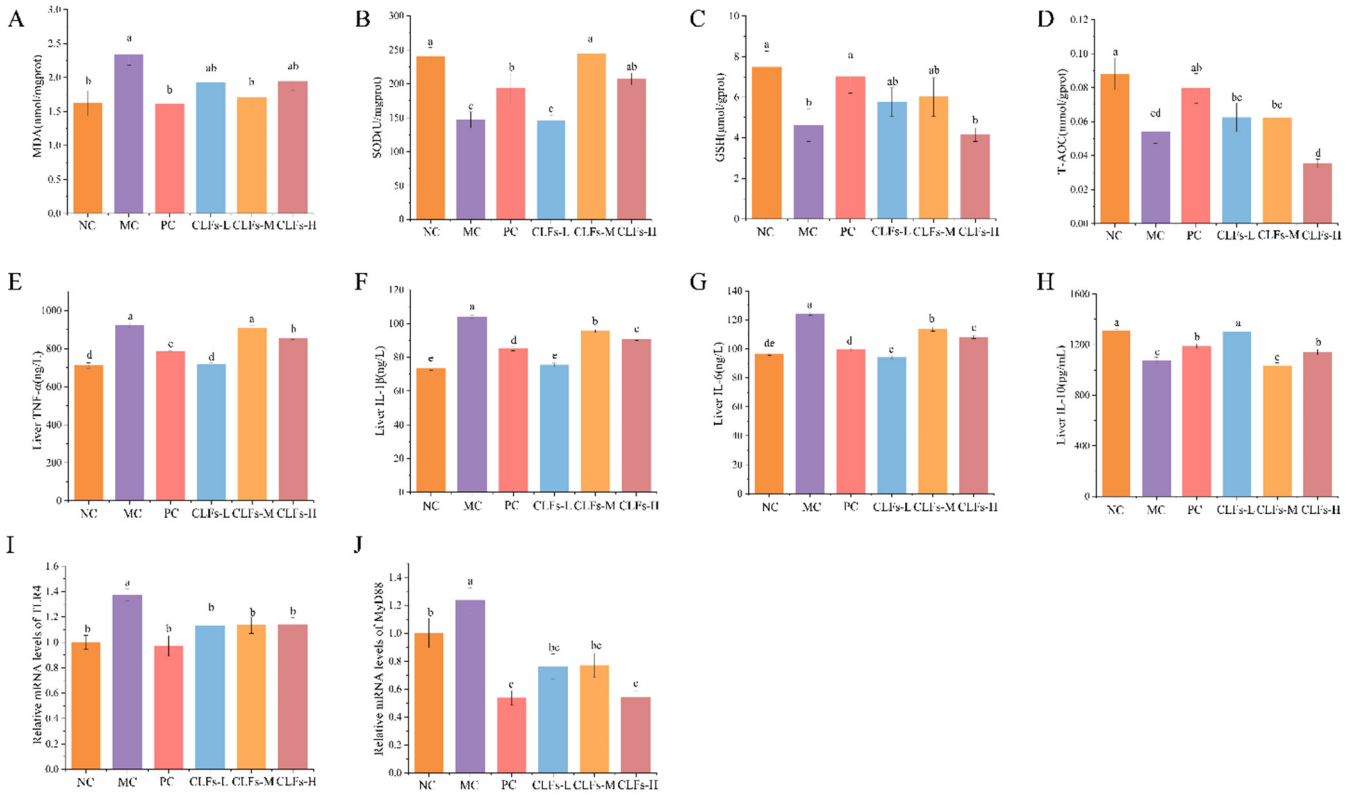

Figure 4 CLFs regulate oxidative stress and liver inflammation levels. (A) Liver MDA; (B) Liver SOD; (C) Liver GSH; (D) Liver T-AOC; (E) Liver TNF-α; (F) Liver IL-1β; (G) Liver IL-6; (H) Liver IL-10. The mRNA expression of TLR4 (I) and MyD88 (J) in the liver was detected by RT-qPCR. Bar charts with different letters indicate significant differences among the six groups ($P < 0.05$), results are expressed as mean ± SE (n = 6).

The levels of liver inflammation in mice are illustrated in Figure 4E-H. While IL-10 levels were significantly lower ($P < 0.05$) in the MC group compared to the NC group, TNF-α, IL-1β, and IL-6 levels were significantly greater, indicating severe liver inflammation. In contrast, compared with the MC group, the levels of TNF-α, IL-1β, and IL-6 were significantly decreased in the CLFs group, and significantly increased levels of IL-10 ($P < 0.05$), with the CLFs-L group exhibiting the lowest levels. This suggests that daily feeding of CLFs can effectively inhibit the excessive reduction of anti-inflammatory cytokines and the excessive expression of pro-inflammatory cytokines in mice with alcoholic liver disease, further validating CLFs' anti-inflammatory activity.

Alcohol induction increased the expression of TLR4 and MyD88 mRNA in mouse livers compared to the NC group (Figure 4I-J). This suggests that the NF-κB pathway was activated in the MC group mice's livers, which could be the main reason for the large release of inflammatory markers in the liver. After CLFs intervention, the expression of TLR4 and MyD88 in mouse livers decreased, suggesting that CLFs can

inhibit the activation of the NF-κB signaling pathway by regulating the expression of upstream genes, thereby reducing the chain reaction of inflammatory pathways and suppressing the occurrence of alcohol-induced liver inflammation in mice.

3.5 CLFs alter the levels of metabolites in the livers of ALD mice

A total of 615 liver metabolites were identified in the experimental group (Figure 5A), including lipids and fatty acids (26.2%), organic acids and derivatives (24.9%), and organic heterocyclic compounds (22.3%). The close clustering of the quality control (QC) samples suggests consistent data, stable conditions, and repeatable outcomes (Figure 5B-C). The OPLS-DA plot demonstrated that CLFs significantly impacted the amounts of liver metabolites in mice, with varying categorization scores among the six groups (Figure 5D). Alcohol impacts normal liver metabolism in mice, as evidenced by 320 metabolites that showed substantial differential expression between the MC and NC groups (VIP > 1 and $P < 0.05$), with 167 metabolites considerably upregulated and 153 metabolites significantly downregulated. With 98 metabolites significantly up-regulated and 87 significantly down-regulated (Figure 5E), the CLFs-H group displayed the most differences when compared to the MC group. This suggests that CLFs-H may dramatically alleviate liver metabolic abnormalities brought on by alcoholic liver disease.

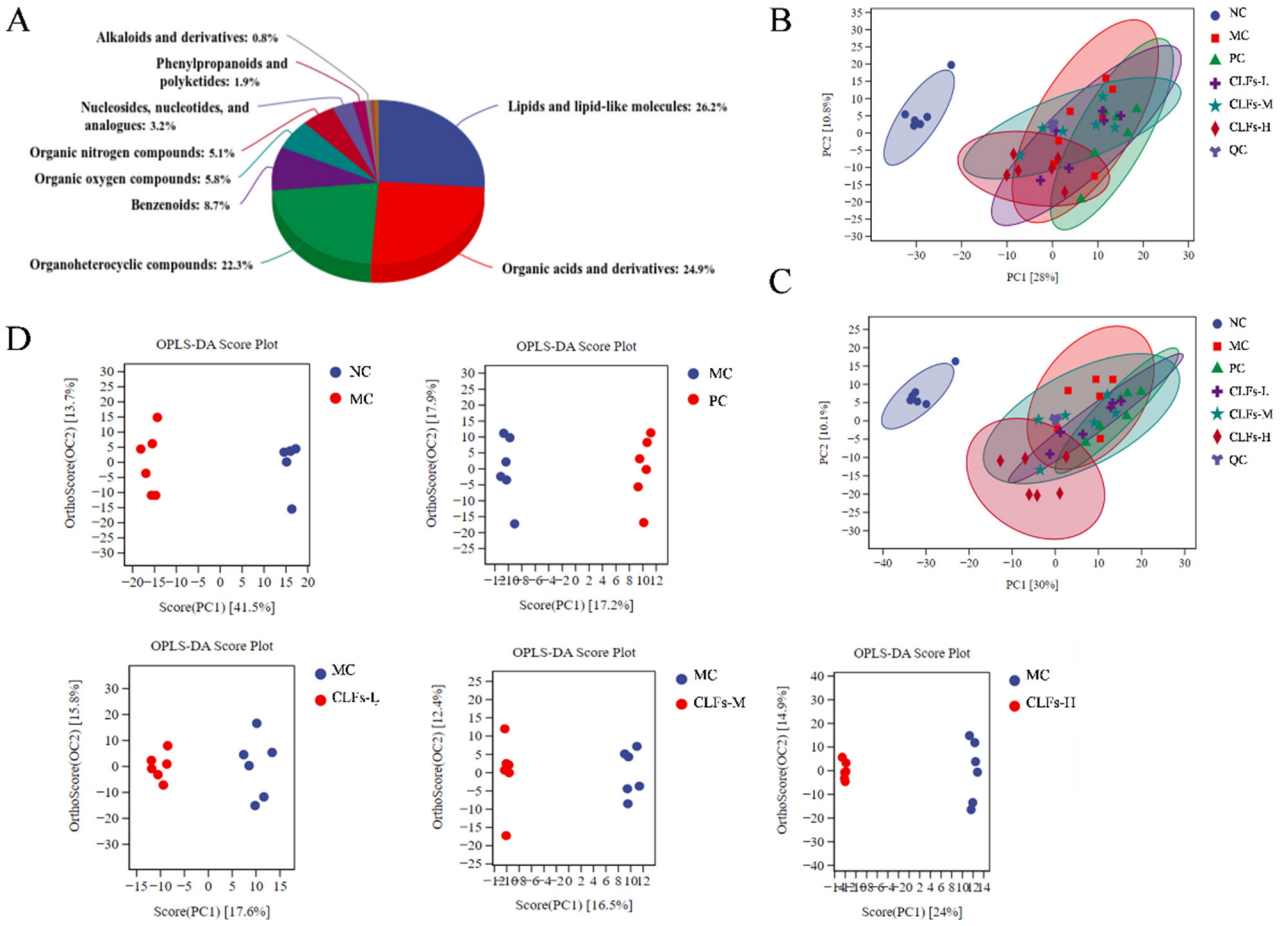

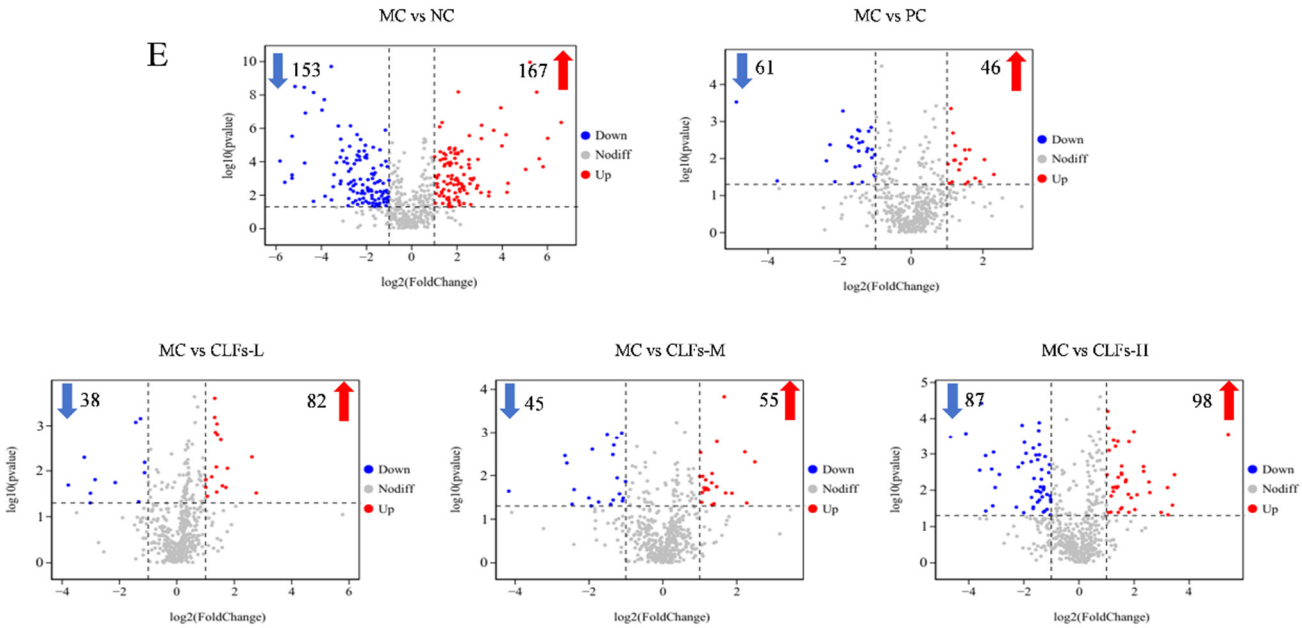

Figure 5 (A) Proportion of identified metabolites in each chemical category. (B) PCA score plot in positive mode. (C) PCA score plot in negative mode. (D) OPLS-DA score plot comparing the MC group with the NC, PC, CLFs-L, CLFs-M, and CLFs-H groups. (E) Volcano plot of differentially expressed metabolites. Metabolites meeting the criteria of FC > 1 and *P* value < 0.05 are shown in red, while those meeting FC < 1 and *P* value < 0.05 are shown in blue. Non-significant metabolites are shown in gray.

3.6 CLFs Improve Alcoholic Liver Disease in Mice Through the Nrf2/HO-1 Pathway

It was concluded that alcohol consumption reduced the levels of the metabolites L-tryptophan and L-glutamine in comparison to the NC group by combining the findings of the KEGG pathway enrichment analysis and the differential metabolite heatmap analysis. Additionally, the digestive system, protein and mineral absorption, and amino acid metabolism were the main topics of the top 20 metabolic pathways found. This study primarily looked at the glutathione metabolism and tryptophan metabolism. The pathway for glutathione metabolism was highly enriched, ranking only behind that of mineral absorption and ABC transporters (Figure 6A-B). Combining non-targeted liver metabolomics with previous research findings, CLFs may improve alcoholic liver disease through the Nrf2/HO-1 oxidative stress pathway. The Nrf2/HO-1 signaling pathway was confirmed by the detection of Nrf2 and HO-1 protein expression levels, as well as Keap1, Nrf2, NQO-1, and HO-1 mRNA expression levels. The RT-qPCR results showed that following alcohol consumption, the MC group's mRNA levels of Keap1 dramatically increased, whereas those of Nrf2, NQO-1 and HO-1 significantly dropped (Figure 6C-F). The aberrant mRNA expression brought on by alcoholic liver disease was reversed to differing degrees by CLFs at various dosages. Similarly, the MC group showed a significant decrease in the levels of Nrf2 and HO-1 protein expression, whereas CLFs boosted both Nrf2 and HO-1 protein expression (Figure 6G-I). This implies that CLFs protect liver function by activating the Nrf2/HO-1 signaling pathway, which helps maintain the body's redox system equilibrium.

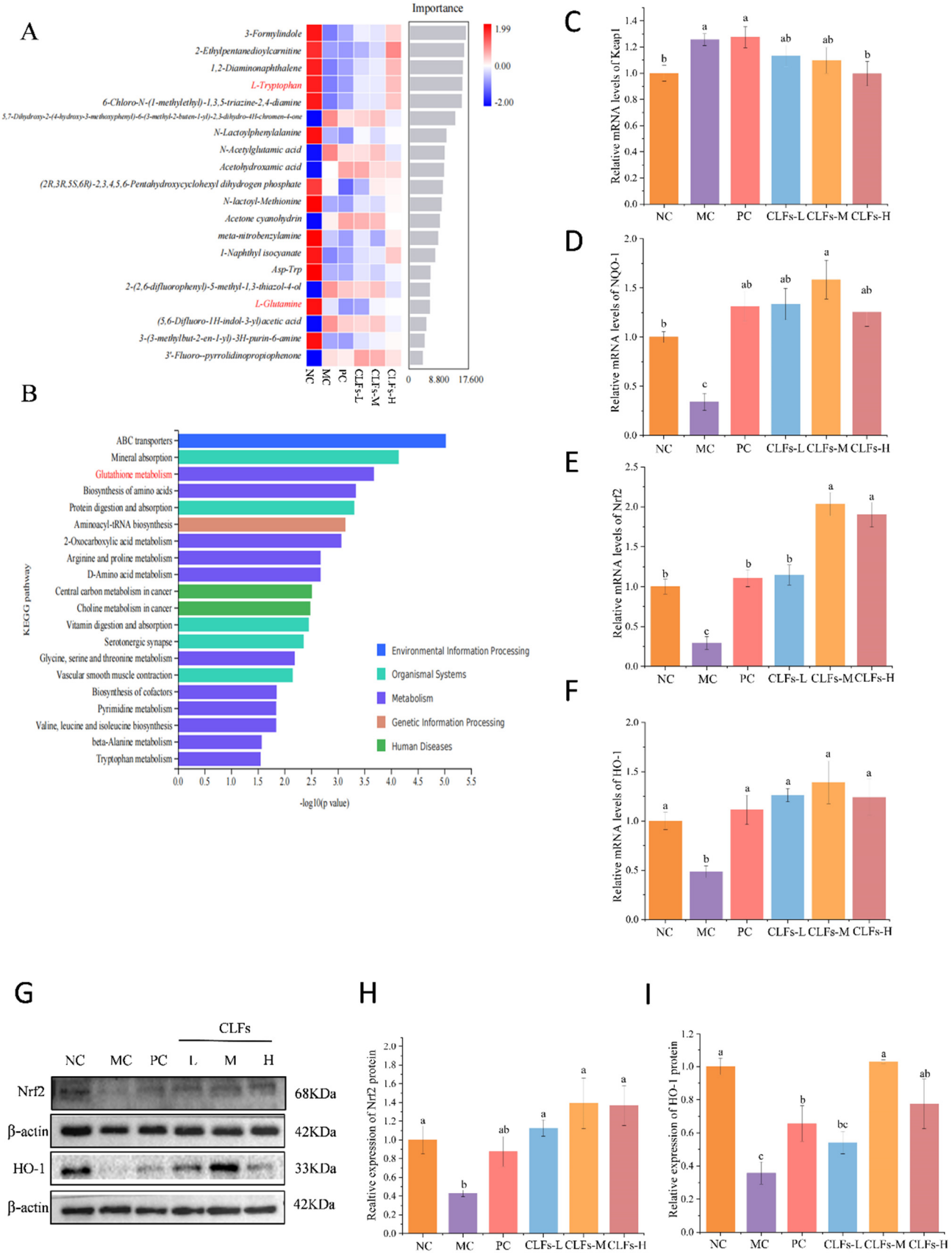

Figure 6 CLFs activate the Nrf2/HO-1 signaling pathway to regulate liver metabolism. Results are expressed as mean ± SE. (A) Heatmap of different liver metabolites among groups; (B) Bar chart of KEGG enriched metabolic pathways of liver metabolites with significant differences between CLFs-H-treated and ALD mice (n=6). The mRNA expression of Keap1 (C), Nrf2 (D), NQO-1 (E) and HO-1 (F) in the liver was detected by RT-qPCR (n=6). (G) Representative western blot image. The protein expression of Nrf2 (H) and HO-1 (I) in the liver was detected by Western blotting (n=3). Bar charts with different letters indicate significant differences among the six groups ($P < 0.05$).

3.7 CLFs Protect Intestinal Barrier Integrity in ALD Mice

As shown in Figure 7A, the MC group demonstrated a depletion of cup cells and a deficiency of mucus compared to the NC group. Glycogen levels and the quantity of cup cells rose following CLFs administration, suggesting that CLFs may help repair intestinal damage brought on by alcohol. Compared with the NC group, the levels of TNF-α, IL-1β, and IL-6 in the colon tissue of the MC group were significantly elevated, while the level of IL-10 was significantly reduced ($P < 0.05$). CLFs therapy decreased TNF-α, IL-1β, and IL-6 levels while increasing IL-10 levels compared to the MC group (Figures 7C-F). Alcohol intake led to significantly higher serum LPS levels in the MC group compared to the NC group ($P < 0.05$). However, after CLFs intervention, serum LPS levels in mice were reduced to varying degrees, with significant differences compared to the MC group (Figure 7B), indicating that alcohol disrupts the intestinal barrier in mice, while CLFs activate the immune response, regulate immune cell levels, and enhance immune barrier function.

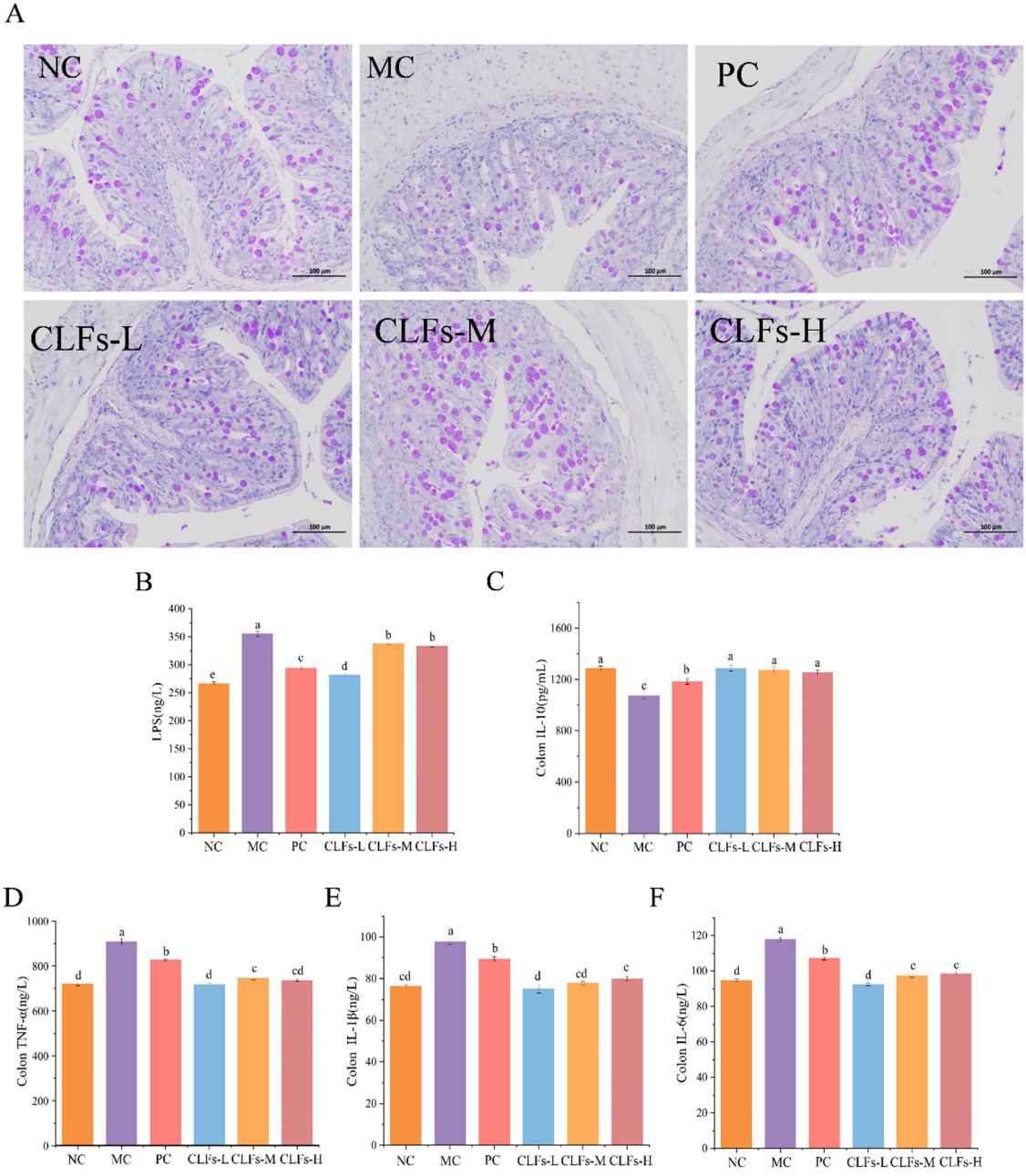

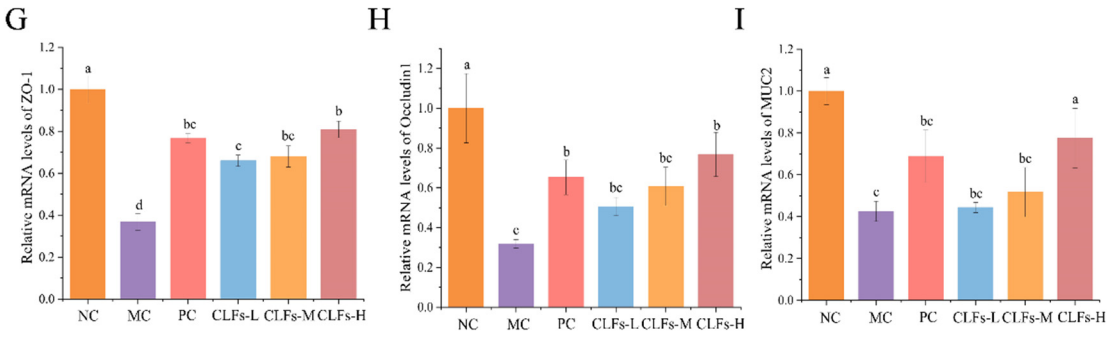

Figure 7 CLFs protect the intestinal barrier of ALD mice. Results are expressed as mean ± SE.(A) PAS staining of colon tissue; (B) Serum LPS; (C) Colon IL-10; (D) Colon TNF-α; (E) Colon IL-1β; (F) Colon IL-6. The mRNA expression of ZO-1(G), Occludin1 (H) and MUC2 (I) in the colon was detected by RT-qPCR. Bar charts with different letters indicate significant differences among the six groups ($P < 0.05$), results are expressed as mean ± SE (n = 6).

As shown in Figure 7G-I, alcohol consumption led to a significant decrease in the mRNA levels of ZO-1, Occludin1, and MUC2 in mouse intestinal tissue ($P < 0.05$). ZO-1, Occludin1, and MUC2 mRNA levels all markedly rose after high-dose CLFs intervention, suggesting that CLFs restored intestinal function from the standpoints of the mechanical and chemical barriers. Thus, it is both possible and promising to investigate the preventive effects of CLFs on alcoholic liver disease from the standpoint of maintaining the integrity of the intestinal barrier function.

3.8 CLFs Restore Intestinal Microbiota Balance in ALD Mice

The findings of the Chao1 index, Shannon index, Goods coverages, and Observed species index showed that CLFs significantly increased the species abundance and diversity of the gut microbial community when compared to the MC group (Figure 8C). The MC group and the NC group were clearly divided geographically, with some distance differences, according to principal component analysis (PCA) and non-metric multidimensional scaling analysis (NMSD) analysis based on the Bray-Curtis distance algorithm. Both groups also moved closer to the NC group to varying degrees following CLFs supplementation (Figure 8D-E). There were 286 OTUs that overlapped among the six groups. Furthermore, after CLFs supplementation, the number of OTUs rose in all groups, but the MC group exhibited the fewest distinct microbial communities (Figure 8G).

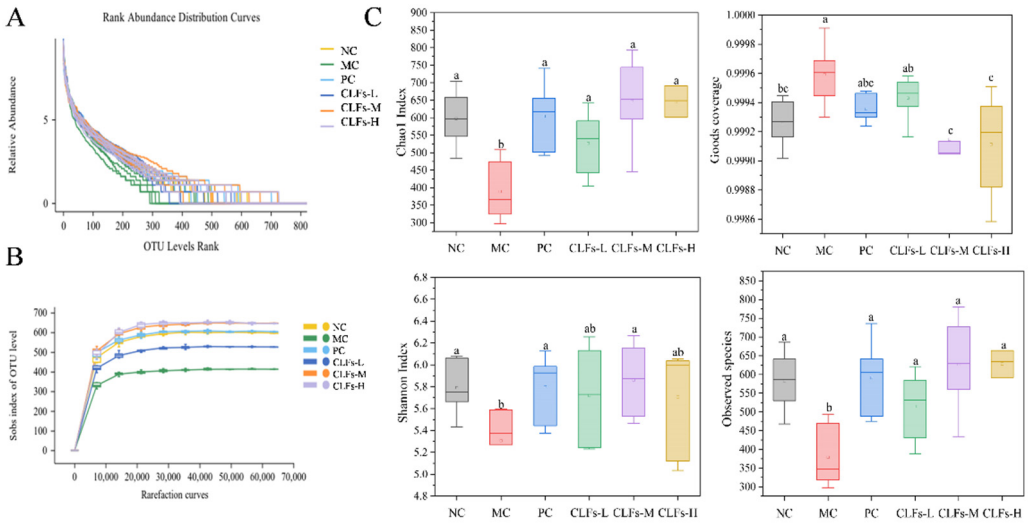

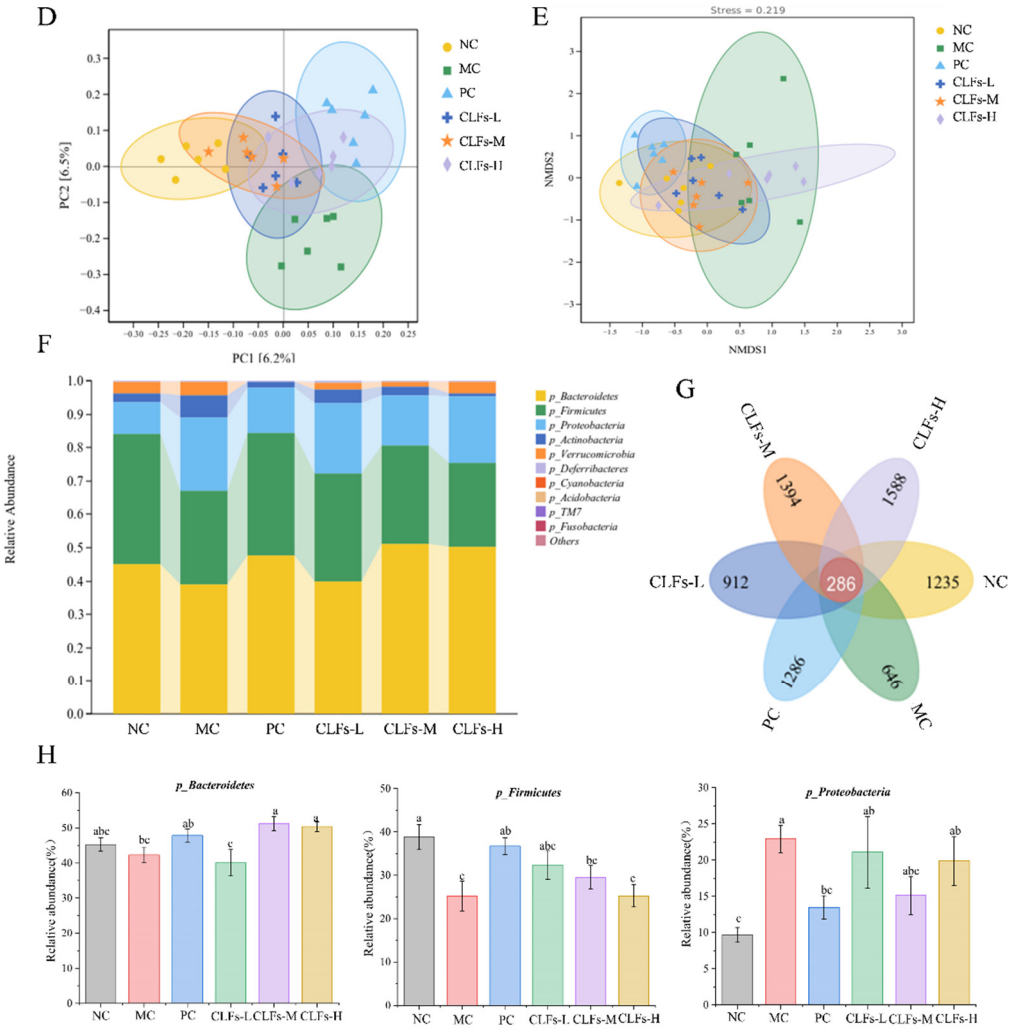

Figure 8 (A) Rank-Abundance curve of gut microbiota in ALD mice; (B) Rarefaction curve; (C) α diversity analysis of gut microbiota in ALD mice; (D) Principal component analysis (PCA); (E) Non-metric multidimensional scaling analysis (NMSD); (F) Histogram of the distribution of abundance and composition of the top 10 phyla-level cecal microbiota; (G) Venn diagram; (H) Changes in the relative abundance of the *p-Bacteroidetes, p-Firmicutes, and p-Proteobacteria.* Bar charts with different letters indicate significant differences among the six groups ($P < 0.05$, n = 6).

At the phylum level, the *p-Firmicutes*, *p-Bacteroidetes*, and *p-Proteobacteria* played important roles in the gut microbiota of all groups. Among these, the proportions of *p-Firmicutes* and *p-Bacteroidetes* both exceeded 60% (Figure 8F). Compared with the NC group, the *p-Firmicutes* was significantly reduced, the *p-Proteobacteria* was significantly increased, and the *p-Bacteroidetes* was slightly reduced but without a significant difference in the MC group, indicating that alcohol induction exacerbates the occurrence of intestinal inflammation. After CLFs intervention, the abundance of the *p-Firmicutes* and *p-Bacteroidetes* increased, while the abundance of the *p-Proteobacteria* decreased, suggesting that CLFs reduce the likelihood of pathogenic bacteria harming the intestinal microbiota (Figure 8H). At the genus level, the *g-Parabacteroides* and *g-Bacteroides* play important roles in all groups. Compared with the NC group, the relative abundance of the *g-Parabacteroides* and *g-Clostridium-f-Clostridiaceae* decreased in the MC group, while the relative abundance of the *g-Bacteroides* increased. This trend was reversed with CLFs intervention (Figure 9A-B). In summary, CLFs can effectively regulate the abundance of the intestinal microbiota at the genus level.

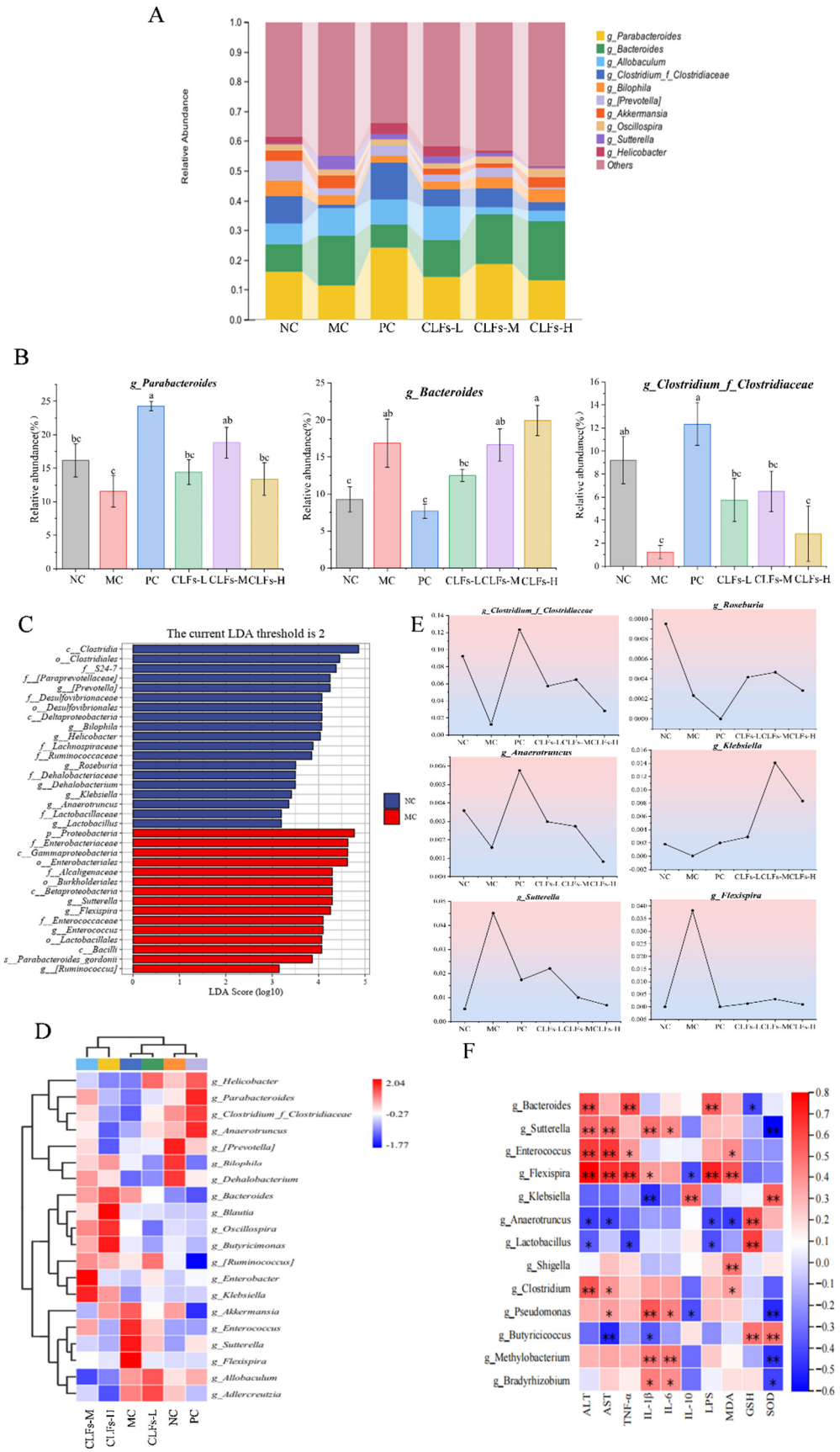

Figure 9 (A) Histogram of the distribution of genus-level microbial community abundance and composition in the cecum; (B) Changes in the relative abundance of *g-Probacteroides,g-Prevotella,* and *g_Clostridium_f_Clostridiaceae* (C) LDA classification bar chart based on the NC and MC groups (LDA > 2); (D) Heatmap of gut microbiota composition at the genus level; (E) Changes in the abundance of 6 potential bacterial genera; (F) Correlation analysis between biochemical indicators and gut microbiota. Bar charts with different letters indicate significant differences among the six groups ($P < 0.05$), results are expressed as mean ± SE (n = 6).

LEfSe analysis was carried out on the NC and MC groups to investigate the possible microbiota that is in charge of the positive effects of CLFs in mice with alcohol-induced liver damage. According to the findings, the MC group were enriched with two possibly hazardous bacteria, *g-Sutterella* and *g-Flexispira*, whereas the NC group was enriched with four potentially advantageous bacteria, *g-Clostridium-f-Clostridiaceae, g-Roseburia, g-Anaerotruncus*, and *g-Klebsiella*. To confirm the validity of the previously mentioned potential bacterial genera and to identify notable differences in bacterial genera across low, medium, and high doses, a heatmap analysis was performed to examine changes in the abundance of intestinal microbiota composition at the genus level. All six selected potential bacterial genera were reflected in the heatmap, demonstrating a positive correlation with the NC group and treatment group and a negative correlation with the MC group, further confirming that these bacteria are potential beneficial or harmful bacteria (Figure 9C-D). The relative abundance changes of these six putative bacterial taxa across the groups are shown in Figure 9E. While *g-Clostridium_f-Clostridiaceae* and *g-Anaerotruncus* showed a negative correlation with ALT and AST, *g-Sutterella, g-Enterococcus* and *g-Flexispira* showed a favorable correlation (Figure 9F). These results suggest that CLFs may improve alcoholic liver disease by regulating the relative abundance of *g-Clostridium-f-Clostridiaceae, g-Roseburia, g-Anaerotruncus, g-Klebsiella, g-Sutterella* and *g-Flexispira.*

4. Discussion

In this study, CLFs were extracted and purified from *C. salicifolius* leaves. Its principal constituents include rutin, hyperoside, isoquercitrin, luteoloside, kaempferol-3-O-rutinoside and astragalin. The results indicate that CLFs exhibit strong antioxidant activity. Its phenolic hydroxyl group has a strong affinity for hydrogen atoms or neutrons, and has antioxidant and protective effects against oxidative damage to biological tissue membranes and DNA caused by free radicals[29]. Some studies have shown that rutin can play an important role in improving cell membrane damage and preventing cell apoptosis, showing a protective effect on alcohol induced liver cell damage[30], at the same time, it can promote hepatocyte proliferation, reduce blood glucose level, and stimulates insulin production to improve type 2 diabetes[31]; kaempferol can inhibit bile acid synthesis by targeting the intestinal FXR-FGF15 signaling pathway, thereby improving alcoholic liver disease[32]. Therefore, CLFs has demonstrated superior bioactive effects, which may be attributed to its high content of rutin and kaempferol-3-O-rutinoside.

The liver is the primary organ responsible for alcohol metabolism. Metabolic products generated during alcohol metabolism can cause liver damage and lead to ALD through various mechanisms, such as damage to lipid metabolism, exacerbation of inflammatory responses, and induction of fibrosis[33]. ALT and AST have traditionally been considered markers of liver cell damage[34]. When the liver is damaged, substances in the cells easily leak into the bloodstream, causing elevated levels of ALT and AST in the serum[35]. Excessive alcohol use causes lipid metabolism problems and fatty degeneration in the liver due to the accumulation of alcohol and its metabolites[36]. Abnormal metabolism of total cholesterol and triglycerides is typically associated with disorders of lipid transport proteins[37]. In ALD mice, CLFs can reduce the levels of

serum biomarkers, inhibit the expression of TC and TG, and reverse liver lipid peroxidation levels. Meanwhile, the H&E staining results indicate that CLFs treatment can alleviate severe hepatic steatosis and reduce the occurrence of fat vacuoles, consistent with previous findings[35].

Oxidative stress is a major contributing factor to alcoholic liver injury[38]. The antioxidant enzymes SOD and lipid peroxidation marker MDA are generally used to evaluate oxidative stress levels. While SOD, GSH, and T-AOC levels dramatically decreased in mouse liver tissue following alcohol induction, MDA levels greatly increased, suggesting increased oxidative stress and lipid peroxidation. CLFs exhibited good antioxidant activity, significantly reducing MDA levels while significantly increasing SOD, GSH, and T-AOC levels, thereby improving the body's antioxidant capacity.

Alcohol can cause liver damage via triggering the immune system and dendritic cells in the liver, as well as by causing TNF-α to be produced. After alcohol stimulation, lipopolysaccharide (LPS) produced by intestinal bacteria enters the bloodstream, travels through the portal vein system into the liver, binds to toll-like receptor (TLR)-4, activates dendritic cells, and initiates the TLR4-mediated signaling pathway. Toll-like receptors (TLRs) serve as a bridge between innate and adaptive immunity, mediating signal transduction pathways through the myeloid differentiation primary response protein 88 (MyD88)-dependent pathway. Alcohol consumption leads to a significant increase in LPS levels in the MC group mice, but CLFs intervention helps ALD mice restore normal levels of inflammatory factors in the liver and downregulate the expression of TLR4/MyD88 inflammatory signaling pathway.

The intestinal mucosal barrier is crucial for maintaining gastrointestinal homeostasis, which is composed of physical barrier, chemical barrier, immune barrier, and microbial components[39]. Long-term excessive alcohol consumption not only damages the liver but also disrupts the integrity of the intestinal wall[40]. PAS staining results demonstrate that alcohol-induced disruption of the intestinal barrier occurs. The physical barrier is mainly composed of intestinal epithelial cells and is a dynamic and permeable barrier with bidirectional barrier function, allowing nutrients to enter the body while preventing pollutants such as bacteria and endotoxins from entering the bloodstream. Intestinal permeability is determined by tight junction proteins, which are important molecular components of the intestinal mucosal barrier[41]. The chemical barrier includes the mucus secreted by cup cells, which mainly secretes mucin called MUC2, which can prevent bacteria from damaging the chemical barrier of epithelial cells and help protect the intestinal mucosal barrier. TNF-α, IL-1β, IL-6, and IL-10 are important inflammatory cytokines involved in various physiological processes, including host defense, inflammation, cancer, and immune diseases[42]. After intervention with CLFs, the mRNA levels of ZO-1, Occludin1, and MUC2 significantly increased, while reducing the levels of pro-inflammatory factors TNF - α, IL-1 β, and IL-6 and increasing the level of anti-inflammatory factor IL-10. This indicates that CLFs can maintain the integrity of intestinal barrier function by enhancing the intestinal barrier and regulating immune responses.

Recent studies have shown that gut microbiota dysbiosis plays a crucial role in the onset and progression of ALD. Alcohol consumption disrupts the structure and composition of the gut microbiota,

leading to gut microbiota dysbiosis[43]. In this study, 16S rRNA sequencing revealed that CLFs reshapes gut microbiota composition. *Proteobacteria* is a pro-inflammatory bacterium that can multiply in the gut and lead to microbial community imbalance, whereas alterations in the *Firmicutes* and *Bacteroidetes* are frequently seen as indicators of gut microbial health in terms of gut microbiota composition[44]. At the phylum level, *Bacteroidetes* and *Firmicutes* played an advantageous role. Alcohol consumption led to an increase in the abundance of the harmful *p-Proteobacteria* and a decrease in the abundance of the beneficial *p-Firmicutes* in the MC group. Studies have shown that the *g-Parabacteroides* possesses physiological characteristics related to carbohydrate metabolism and the secretion of short-chain fatty acids[45]. In addition to providing intestinal epithelial cells with energy, the short-chain fatty acids (SCFAs) produced by the *Clostridium* family can also control secondary BA metabolism, trigger regulatory immunological responses, and create IgA[46]. Alcohol abuse is also considered a major cause of reduced *Clostridium* levels[47]. *Roseburia* is a butyrate-producing bacterium that can reduce intestinal permeability and decrease the production of pro-inflammatory factors. *Anaerotruncus* is linked to energy metabolism and is a member of the group of bacteria that produce short-chain fatty acids[48]. All of these bacterial genera can alleviate alcohol-induced liver disease by improving intestinal barrier function. The anti-inflammatory and immunomodulatory effects of CLFs may therefore be associated with a reduction in the abundance of harmful bacteria such as *g-Sutterella*, *g-Enterococcus*, and *g-Flexispira*, as well as an increase in the abundance of beneficial bacteria such as *g-Bacteroides, g-Clostridium-f-Clostridiaceae, g-Roseburia,* and *g-Anaerotruncus*. In addition, correlation analysis showed a significant correlation between gut microbiota and serum indicators, liver antioxidant capacity, and inflammation, indicating that CLFs mediated microbiota remodeling helps alleviate liver injury.

As the largest gland in the human body, the liver performs numerous amazing biological functions[49]. It establishes a communication bridge between the portal vein system and the intestine, known as the "gut-liver axis", which has the function of regulating the intestine, affecting liver metabolism, energy storage, and detoxification[50]. It is crucial to analyze the protective mechanisms of CLFs against alcohol-induced intestinal and liver damage based on the “gut-liver axis”. In this study, non-targeted metabolomics analysis was performed on liver tissue from ALD mice. Notably, two pathways, tryptophan metabolism and glutathione metabolism, were identified in the KEGG enrichment pathways. Alcohol exposure activates the kynurenine pathway of tryptophan metabolism, activating indoleamine 2,3-dioxygenase 1 (IDO1) enzyme, and results in tryptophan depletion. This process produces metabolites 3-hydroxycarnitine (3-HK) and further degrades into quinolinic acid (QA), which consumes NAD+ and damages mitochondrial function, leading to an increase in ROS[51]. Liver function is hampered concurrently by increased ROS generation due to compromised mitochondrial activity[52]. IDO-mediated metabolism may further induce oxidative stress, because tryptophan and oxygen seem to interact by forming an intermediate molecule that could be a potent oxidizing agent[53]. Endogenous antioxidants like glutathione

(GSH)/GSH-peroxidase system and exogenous antioxidants like polyphenols can mitigate the negative effects of ROS produced by the IDO reaction[54].

Glutathione is the main antioxidant that regulates cellular redox balance, and the liver is primarily responsible for its production and metabolism[55-56]. It affects several cellular processes, including fibrosis, immune system modulation, cell cycle regulation, detoxification of foreign chemicals and xenobiotics, and antioxidant defense[57]. Glutathione S-transferase (GST) contributes to the body's antioxidant reactions by catalyzing the metabolism of glutathione (GSH), binding to, and eliminating endogenous or foreign electrophilic substances[58]. Excessive alcohol use activates cytochrome P4502E1 (CYP2E1), which produces toxic reactive oxygen species (ROS) and consumes liver GSH levels[59-60]. The depletion of GSH can lead to ineffective clearance of acetaldehyde and ROS, exacerbating oxidative stress levels in the body and causing greater damage to the liver. Therefore, it is speculated that CLFs may enhance the body's antioxidant capacity by regulating tryptophan metabolism and glutathione metabolism, thereby alleviating the damage caused by alcohol to the body.

The Nrf2/HO-1 signaling pathway is closely associated with oxidative stress, and its expression levels reflect the extent of oxidative stress[61]. Nrf2 has been confirmed to be a core transcription factor in the antioxidant defense system. Under normal conditions, Nrf2 tightly binds to Keap1 and undergoes ubiquitination and degradation in the cytoplasm[62]. When oxidative stress occurs, Nrf2 dissociates from Keap1 and enters the nucleus, binding to the antioxidant response element (ARE) to promote the expression of downstream antioxidant genes such as HO-1 and NQO-1, thereby regulating oxidative stress damage and inhibiting apoptosis[63]. Therefore, combined with previous measurements of oxidative stress markers, further RT-qPCR and Western Blotting experiments validated the presence of the Nrf2/HO-1 signaling pathway. In an alcohol-induced mouse model, CLFs can regulate the body's oxidative stress levels, modulate Keap1, NQO-1, Nrf2, and HO-1 mRNA expression, while activating the Nrf2/HO-1 signaling pathway, significantly enhancing the expression of Nrf2 and its downstream antioxidant proteins. This suggests that the regulation of the Nrf2/HO-1 pathway may be the key mechanism by which CLFs exert their liver protective effects.

In this study, it has been demonstrated that CLFs can regulate its oxidative stress levels through the Nrf2/HO-1 signaling pathway, alleviate inflammatory responses, maintain gut microbiota homeostasis, and modulate metabolic pathways to protect against alcohol-induced liver damage. Nevertheless, there are still some restrictions on our study. First, LC-MS experiments can be further supplemented to ensure the accuracy of the results. Second, this study only explored the effects from the perspective of oxidative stress. In future research, the multi-target and multi-pathway advantages of *C. salicifolius* leaves flavonoids can be elucidated by constructing fecal microbiota transplantation models or combining transcriptomics and proteomics for multi omics integrated analysis.

5. Conclusion

CLFs showed excellent antioxidant activity *in vitro* and alleviated the symptoms of alcoholic liver disease in mice *in vivo*. The protective effect of CLFs against alcohol-induced liver disease is primarily attributed to their regulation of oxidative stress levels through the Nrf2/HO-1 signaling pathway, inhibition of inflammatory responses, adjustment of gut microbiota metabolism, and maintenance of the intestinal barrier to protect ALD mice from liver damage. In conclusion, our research provides experimental support for CLFs as a possible therapeutic target for ALD treatment in the future by illuminating the possible mechanisms through which CLFs treat alcoholic liver diseases.

Conflict of interest

The authors declare that they have no known competing financial interests or personal relationships that could have appeared to influence the work reported in this paper.

Acknowledgements

This work was supported by grants from National Natural Science Foundation of China (31560459), Major Discipline Academic and Technical Leaders Training Program of Jiangxi Province (20182BCB22003) and the Earmarked Fund for Jiangxi Agriculture Research System (JXARS-13).

References

[1] H. Kawaratani, K. Moriya, T. Namisaki, et al., Therapeutic strategies for alcoholic liver disease: Focusing on inflammation and fibrosis (Review). Int J Mol Med 40 (2017) 263-270. https://doi.org/10.3892/ijmm.2017.3015.

[2] E.S. Orman, G. Odena, R. Bataller, Alcoholic liver disease: Pathogenesis, management, and novel targets for therapy. J Gastroenterol Hepatol 28 Suppl 1 (2013) 77-84. https://doi.org/10.1111/ jgh.12030.

[3] C. Pan, Y. Abboud, A. Chitnis, et al., Alcohol-associated liver disease mortality. JAMA Netw Open 8 (2025) e2514857. https://doi.org/10.1001/jamanetworkopen 2025.14857.

[4] L. Li, S. Xu, W. Wang, et al., Bruceine A alleviates alcoholic liver disease by inhibiting AIM2 inflammasome activation via activating FXR. Phytomedicine 130 (2024) 155693. https://doi.org/10.1016/j.phymed.2024.155693.

[5] W. Dunn, V.H. Shah, Pathogenesis of alcoholic liver disease. Clin Liver Dis 20 (2016) 445-56. https://doi.org/10.1016/j.cld.2016.02.004.

[6] H. Cichoz-Lach, A. Michalak, Oxidative stress as a crucial factor in liver diseases. World J Gastroenterol 20 (2014) 8082-91. https://doi.org/10.3748/wjg.v20.i25.8082.

[7] J.S. Bajaj, Alcohol, liver disease and the gut microbiota. Nat Rev Gastroenterol Hepatol 16 (2019) 235-246. https://doi.org/10.1038/s41575-018-0099-1.

[8] A. Albillos, A. de Gottardi, M. Rescigno, The gut-liver axis in liver disease: Pathophysiological basis for therapy. J Hepatol 72 (2020) 558-577. https://doi.org/10.1016/j.jhep.2019.10.003.

[9] L. Tedesco, G. Corsetti, C. Ruocco, et al., A specific amino acid formula prevents alcoholic liver disease in rodents. Am J Physiol Gastrointest Liver Physiol 314 (2018) G566-G582. https://doi.org/10.1152/ajpgi.00231.2017.

[10] C. Liu, Y. Wang, L. Sheng, et al., 3-Hydroxypropionaldehyde modulates tryptophan metabolism to activate AhR signaling and alleviate ethanol-induced liver injury. Phytomedicine 139 (2025) 156445. https://doi.org/10.1016/j.phymed.2025.156445.

[11] S. Gao, J. Shi, K. Wang, et al., Protective effects of oyster protein hydrolysates on alcohol-induced liver disease (ALD) in mice: Based on the mechanism of anti-oxidative metabolism. Food Funct 13 (2022) 8411-8424. https://doi.org/10.1039/d2fo00660j.

[12] M. Pellegrinotti, F.L. Fimognari, A. Franco, et al., Erlotinib-induced hepatitis complicated by fatal lactic acidosis in an elderly man with lung cancer. Ann Pharmacother 43 (2009) 542-5. https://doi.org/10.1345/aph.1L468.

[13] X. Forns, F. Poordad, M. Pedrosa, et al., Ombitasvir/paritaprevir/r, dasabuvir and ribavirin for cirrhotic HCV patients with thrombocytopaenia and hypoalbuminaemia. Liver Int 35 (2015) 2358-62. https://doi.org/10.1111/liv.12931.

[14] C. Colombo, P.M. Battezzati, M. Podda, et al., Ursodeoxycholic acid for liver disease associated with cystic fibrosis: A double-blind multicenter trial. The Italian Group for the Study of Ursodeoxycholic Acid in Cystic Fibrosis. Hepatology 23 (1996) 1484-90. https://doi.org/10.1002/hep.510230627.

[15] S. Allampati, K.D. Mullen, Long-term management of alcoholic liver disease. Clin Liver Dis 20 (2016) 551-62. https://doi.org/10.1016/j.cld.2016.02.011.

[16] X. Hong, S. Huang, H. Jiang, et al., Alcohol-related liver disease (ALD): Current perspectives on pathogenesis, therapeutic strategies, and animal models. Front Pharmacol 15 (2024) 1432480. https://doi.org/10.3389/fphar.2024.1432480.

[17] B. Van De Wier, G.H. Koek, A. Bast, et al., The potential of flavonoids in the treatment of non-alcoholic fatty liver disease. Crit Rev Food Sci Nutr 57 (2017) 834-855. https://doi.org/10.1080/10408398.2014.952399.

[18] L. Zhao, Y. Wang, J. Liu, et al., Protective effects of genistein and puerarin against chronic alcohol-induced liver injury in mice via antioxidant, anti-inflammatory, and anti-apoptotic mechanisms. J Agric Food Chem 64 (2016) 7291-7. https://doi.org/10.1021/acs.jafc.6b02907.

[19] A. Rodriguez-Mateos, D. Vauzour, C.G. Krueger, et al., Bioavailability, bioactivity and impact on health of dietary flavonoids and related compounds: An update. Arch Toxicol 88 (2014) 1803-53. https://doi.org/10.1007/s00204-014-1330-7.

[20] X. Liang, C. Zhao, W. Su, A fast and reliable UPLC-PAD fingerprint analysis of *Chimonanthus salicifolius* combined with chemometrics methods. J Chromatogr Sci 54 (2016) 1213-9. https://doi.org/10.1093/chromsci/bmw053.

[21] Y. Zhang, Y. Han, J. He, et al., Digestive properties and effects of *Chimonanthus nitens Oliv.* polysaccharides on antioxidant effects in vitro and in immunocompromised mice. Int J Biol Macromol 185 (2021) 306-316. https://doi.org/10.1016/j.ijbiomac.2021.06.114.

[22] X. Ye, Q. An, S. Chen, et al., The structural characteristics, antioxidant and hepatoprotection activities of polysaccharides from *Chimonanthus nitens Oliv.* leaves. Int J Biol Macromol 156 (2020) 1520-1529. https://doi.org/10.1016/j.ijbiomac.2019.11.200.

[23] W. Meng, L. Chen, K. Ouyang, et al., *Chimonanthus nitens Oliv.* leaves flavonoids alleviate hyperuricemia by regulating uric acid metabolism and intestinal homeostasis in mice. Food Sci. Human Well. 12 (2023) 2440-2450. https://doi.org/10.1016/j.fshw.2023.03.011.

[24] H. Chen, K. Ouyang, Y. Jiang, et al., Constituent analysis of the ethanol extracts of *Chimonanthus nitens Oliv*. leaves and their inhibitory effect on alpha-glucosidase activity. Int J Biol Macromol 98 (2017) 829-836. https://doi.org/10.1016/j.ijbiomac.2017.02.044.

[25] W. Meng, Z. Zhao, L. Chen, et al., Total flavonoids from *Chimonanthus nitens Oliv.* leaves ameliorate HFD-induced NAFLD by regulating the gut-liver axis in mice. Foods 11 (2022). https://doi.org/10.3390/foods11142169.

[26] A. Bertola, S. Mathews, S.H. Ki, et al., Mouse model of chronic and binge ethanol feeding (the NIAAA model). Nat Protoc 8 (2013) 627-37. https://doi.org/10.1038/nprot.2013.032.

[27] X. Li, L. Yang, J. Li, et al., A flavonoid-rich *Smilax china* L. extract prevents obesity by upregulating the adiponectin-receptor/AMPK signaling pathway and modulating the gut microbiota in mice. Food Funct 12 (2021) 5862-5875. https://doi.org/10.1039/d1fo00282a.

[28] Y. Cao, W. Hu, C. Yu, et al., *Cyclocarya paliurus* polysaccharides alleviate hyperuricemia in mice by regulating gut microbiota to enhance uric acid excretion. Int J Biol Macromol 322 (2025) 147029. https://doi.org/10.1016/j.ijbiomac.2025.147029.

[29] J. Garcia-Tirado, C. Rieger-Reyes, P. Saz-Peiro, Effect of flavonoids in the prevention of lung cancer: Systematic review. Med Clin (Barc) 139 (2012) 358-63. https://doi.org/10.1016/j.medcli.2012. 02.003.

[30] Y. Wang, N. Zhang, J. Zhou, et al., Protective effects of several common amino acids, vitamins, organic acids, flavonoids and phenolic acids against hepatocyte damage caused by alcohol. Foods 11 (2022). https://doi.org/10.3390/foods11193014.

[31] W. Liang, D. Zhang, J. Kang, et al., Protective effects of rutin on liver injury in type 2 diabetic db/db mice. Biomed Pharmacother 107 (2018) 721-728. https://doi.org/10.1016/j.biopha.2018.08.046.

[32] L. Xiao, G. Xu, S. Chen, et al., Kaempferol ameliorated alcoholic liver disease through inhibiting hepatic bile acid synthesis by targeting intestinal FXR-FGF15 signaling. Phytomedicine 120 (2023) 155055. https://doi.org/10.1016/j.phymed.2023.155055.

[33] J. Hyun, J. Han, C. Lee, et al., Pathophysiological aspects of alcohol metabolism in the liver. Int J Mol Sci 22 (2021). https://doi.org/10.3390/ijms22115717.

[34] V.L. Chen, X. Du, Y. Chen, et al., Genome-wide association study of serum liver enzymes implicates diverse metabolic and liver pathology. Nat Commun 12 (2021) 816. https://doi.org/10.1038/s41467-020-20870-1.

[35] W. Jiang, H. Zhu, W. Xu, et al., Echinacea purpurea polysaccharide prepared by fractional precipitation prevents alcoholic liver injury in mice by protecting the intestinal barrier and regulating liver-related pathways. Int J Biol Macromol 187 (2021) 143-156. https://doi.org/10.1016/j.ijbiomac. 2021.07.095.

[36] W. Lai, J. Zhang, J. Sun, et al., Oxidative stress in alcoholic liver disease, focusing on proteins, nucleic acids, and lipids: A review. Int J Biol Macromol 278 (2024) 134809. https://doi.org/10.1016/ j.ijbiomac.2024.134809.

[37] Y. Zhou, F. Tan, C. Li, et al., White peony (fermented camellia sinensis) polyphenols help prevent alcoholic liver injury via antioxidation. Antioxidants (Basel) 8 (2019). https://doi.org/10.3390 /antiox 8110524.

[38] I.A. Kirpich, M.E. Miller, M.C. Cave, et al., Alcoholic liver disease: Update on the role of dietary fat. Biomolecules 6 (2016) 1.https://doi.org/10.3390/biom6010001.

[39] T. Rath, R. Atreya, M.F. Neurath, A spotlight on intestinal permeability and inflammatory bowel diseases. Expert Rev Gastroenterol Hepatol 17 (2023) 893-902. https://doi.org/10.1080/ 17474124. 2023.2242772.

[40] T. Shao, C. Zhao, F. Li, et al., Intestinal HIF-1α deletion exacerbates alcoholic liver disease by inducing intestinal dysbiosis and barrier dysfunction. J Hepatol 69 (2018) 886-895. https://doi.org/10.1016/j.jhep.2018.05.021.

[41] J. Xiao, R. Zhang, Y. Wu, et al., Rice bran phenolic extract protects against alcoholic liver injury in mice by alleviating intestinal microbiota dysbiosis, barrier dysfunction, and liver inflammation mediated by the endotoxin-TLR4-NF-κB pathway. J Agric Food Chem 68 (2020) 1237-1247. https://doi.org/10.1021/acs.jafc.9b04961.

[42] Y. Yu, M. Shen, Z. Wang, et al., Sulfated polysaccharide from *Cyclocarya paliurus* enhances the immunomodulatory activity of macrophages. Carbohydr Polym 174 (2017) 669-676. https://doi.org/10.1016/j.carbpol.2017.07.009.

[43] M. Minemura Y. Shimizu, Gut microbiota and liver diseases. World J Gastroenterol 21 (2015) 1691-702. https://doi.org/10.3748/wjg.v21.i6.1691.

[44] N. Shin, T.W. Whon, J. Bae, Proteobacteria: Microbial signature of dysbiosis in gut microbiota. Trends Biotechnol 33 (2015) 496-503. https://doi.org/10.1016/j.tibtech.2015.06.011.

[45] Y. Cui, L. Zhang, X. Wang, et al., Roles of intestinal Parabacteroides in human health and diseases. FEMS Microbiol Lett 369 (2022). https://doi.org/10.1093/femsle/fnac072.

[46] I. Milosevic, A. Vujovic, A. Barac, et al., Gut-liver axis, gut microbiota, and its modulation in the management of liver diseases: A review of the literature. Int J Mol Sci 20 (2019). https://doi.org/10.3390/ijms20020395.

[47] V.B. Dubinkina, A.V. Tyakht, V.Y. Odintsova, et al., Links of gut microbiota composition with alcohol dependence syndrome and alcoholic liver disease. Microbiome 5 (2017) 141. https://doi.org/ 10.1186/s40168-017-0359-2.

[48] L. Chen, Z. Wang, P. Wang, et al., Effect of long-term and short-term imbalanced Zn manipulation on gut microbiota and screening for microbial markers sensitive to Zinc status. Microbiol Spectr 9 (2021) e0048321. https://doi.org/10.1128/Spectrum.00483-21.

[49] A.J. Macpherson, M. Heikenwalder, S.C. Ganal-Vonarburg, The Liver at the nexus of host-microbial interactions. Cell Host Microbe 20 (2016) 561-571. https://doi.org/10.1016/j.chom.2016. 10.016.

[50] S.G. Rodrigues, S. van der Merwe, A. Krag, et al., Gut-liver axis: Pathophysiological concepts and medical perspective in chronic liver diseases. Semin Immunol 71 (2024) 101859. https://doi.org/719 10.1016/j.smim.2023.101859.

[51] A.A. Badawy, Kynurenine pathway of tryptophan metabolism: Regulatory and functional aspects. Int J Tryptophan Res 10 (2017) 1178646917691938. https://doi.org/10.1177/ 1178646917691938.

[52] G. Dogaru, A.E. Bulboaca, D. Gheban, et al., Effect of liposomal curcumin on acetaminophen hepatotoxicity by down-regulation of oxidative stress and matrix metalloproteinases. In Vivo 34 (2020) 569-582. https://doi.org/10.21873/invivo.11809.

[53] N. Le Floc'H, W. Otten, E. Merlot, Tryptophan metabolism, from nutrition to potential therapeutic applications. Amino Acids 41 (2011) 1195-205. https://doi.org/10.1007/s00726-010-0752-7.

[54] K. Hestad, J. Alexander, H. Rootwelt, et al., The role of tryptophan dysmetabolism and quinolinic acid in depressive and neurodegenerative diseases. Biomolecules 12 (2022). https://doi.org/10.3390/ biom12070998.

[55] P. Diaz-Vivancos, A. de Simone, G. Kiddle, et al., Glutathione-linking cell proliferation to oxidative stress. Free Radic Biol Med 89 (2015) 1154-64. https://doi.org/10.1016/j.freeradbiomed. 2015.09.023.

[56] M. Vairetti, L.G. Di Pasqua, M. Cagna, et al., Changes in glutathione content in liver diseases: An update. Antioxidants (Basel) 10 (2021). https://doi.org/10.3390/antiox10030364.

[57] G. Santacroce, A. Gentile, S. Soriano, et al., Glutathione: Pharmacological aspects and implications for clinical use in non-alcoholic fatty liver disease. Front Med (Lausanne) 10 (2023) 1124275. https://doi.org/10.3389/fmed.2023.1124275.

[58] V. Prysyazhnyuk, L. Sydorchuk, R. Sydorchuk, et al., Glutathione-S-transferases genes-promising predictors of hepatic dysfunction. World J Hepatol 13 (2021) 620-633. https://doi.org/10.4254/ wjh.v13.i6.620.

[59] B. Le Dare, V. Lagente, T. Gicquel, Ethanol and its metabolites: Update on toxicity, benefits, and focus on immunomodulatory effects. Drug Metab Rev 51 (2019) 545-561. https://doi.org/10.1080/ 03602532.2019.1679169.

[60] A.I. Cederbaum, Cytochrome P450 2E1-dependent oxidant stress and upregulation of anti-oxidant defense in liver cells. J Gastroenterol Hepatol 21 Suppl 3 (2006) S22-5. https://doi.org/10.1111/j.1440-7481746.2006.04595.x.

[61] L. Yu, H. Li, J. Guo, et al., Di (2-ethyl hexyl) phthalate (DEHP)-induced spleen toxicity in quail (Coturnix japonica) via disturbing Nrf2-mediated defense response. Environ Pollut 251 (2019) 984-989.https://doi.org/10.1016/j.envpol.2019.05.061.

[62] I. Buendia, P. Michalska, E. Navarro, et al., Nrf2-ARE pathway: An emerging target against oxidative stress and neuroinflammation in neurodegenerative diseases. Pharmacol Ther 157 (2016) 84-104. https://doi.org/10.1016/j.pharmthera.2015.11.003.

[63] M.J. Alcaraz, M.L. Ferrandiz, Relevance of Nrf2 and heme oxygenase-1 in articular diseases. Free Radic Biol Med 157 (2020) 83-93. https://doi.org/10.1016/j.freeradbiomed.2019.12.007.